DR. ROBERTO DOCAMPO (Orcid ID : 0000-0003-4229-8784)
DR. SILVIA N J MORENO (Orcid ID : 0000-0002-2041-6295)

Article type : Research Article

Ca^{2+} entry at the plasma membrane and uptake by acidic stores is regulated by the activity of the V-H^+-ATPase in *Toxoplasma gondii*.

Andrew J. Stasic[1], Eric J. Dykes[1,2], Ciro D. Cordeiro[1,2], Stephen A. Vella[1], Mojtaba S. Fazli[3], Shannon Quinn[2,3], Roberto Docampo[1,2], and Silvia N.J. Moreno[1,2]*

[1]Center for Tropical and Emerging Global Diseases and Department of Cellular Biology, University of Georgia, GA 30602-7400.
[2]Department of Cellular Biology, University of Georgia, Athens, GA 30602.
[3]Department of Computer Sciences, University of Georgia, Athens, GA 30602.

*Corresponding author: Silvia NJ Moreno, Department of Cellular Biology, University of Georgia, 350A Coverdell Center, 500 D.W. Brooks Dr. Athens, GA 30602-7399, U.S.A., Phone: (706) 542-4736, E-mail: smoreno@uga.edu

Running title: Vacuolar H^+-ATPase, Ca^{2+} and polyphosphate in *T. gondii*

Keywords: Acidocalcisome, calcium, plant-like vacuole, polyphosphate, *Toxoplasma gondii*, vacuolar H^+-ATPase

Abstract

Ca^{2+} is a universal intracellular signal that regulates many cellular functions. In *Toxoplasma gondii*, the controlled influx of extracellular and intracellular Ca^{2+} into the cytosol initiates a signaling cascade that promotes pathogenic processes like tissue destruction and dissemination. In this work we studied the role of proton transport in cytosolic Ca^{2+} homeostasis and the initiation of Ca^{2+} signaling. We used a *T. gondii* mutant of the V-ATPase, a pump previously shown to transport protons to the extracellular medium, control intracellular pH and membrane potential and we show that proton gradients are important for maintaining resting cytosolic Ca^{2+} at physiological levels and for Ca^{2+} influx. Proton transport was also important for Ca^{2+} storage by acidic stores and, unexpectedly, the endoplasmic reticulum. Proton transport impacted the amount of polyphosphate (polyP), a phosphate polymer that binds Ca^{2+} and concentrate in acidocalcisomes. This was supported by the co-localization of the vacuolar transporter chaperone 4 (VTC4), the catalytic subunit of the VTC complex that synthesizes polyP, with the V-ATPase in acidocalcisomes. Our work show that proton transport regulate plasma membrane Ca^{2+} transport and control acidocalcisome polyP and Ca^{2+} content impacting Ca^{2+} signaling and downstream stimulation of motility and egress in *T. gondii*.

Introduction

Toxoplasma gondii is an Apicomplexan parasite that infects approximately one-third of the world's population. Although usually asymptomatic in healthy adults, death or serious complications from *T. gondii* infections occur in immunocompromised individuals (Ambroise-Thomas & Pelloux, 1993, Holland, 1989, Machala *et al.*, 2015). The pathogenicity of this obligate intracellular parasite is linked to its lytic cycle, which consists of invasion of host cells, replication inside a parasitophorous vacuole (PV), egress resulting in lysis of the host cell, and invasion of a new host cell (Black & Boothroyd, 2000, Blader *et al.*, 2015)

Ca^{2+} signaling is universal and it is involved in a large number of biological functions (Clapham, 2007). In *Toxoplasma*, Ca^{2+} signals triggered by Ca^{2+} influx at the plasma membrane and/or release from intracellular stores start a signaling cascade that culminates in the stimulation of most of the steps of the parasite lytic cycle (Lourido & Moreno, 2015, Hortua Triana *et al.*, 2018). Ca^{2+} influx through a plasma membrane channel was characterized by assessing cytosolic Ca^{2+} concentration ($[Ca^{2+}]_c$) changes following exposure of tachyzoites to high extracellular Ca^{2+}. Ca^{2+} influx into the cytosol is highly regulated presumably by the action of a Ca^{2+} pump at the plasma membrane and by the action of other pumps like the SERCA-Ca^{2+}-ATPase at the endoplasmic reticulum (ER) (Pace *et al.*, 2014).

Toxoplasma gondii tachyzoites, as other eukaryotic cells, maintain their $[Ca^{2+}]_c$ at less than 100 nM. They also possess intracellular Ca^{2+} stores like the ER, and acidic Ca^{2+} stores (Patel & Docampo, 2010), such as acidocalcisomes (Moreno & Zhong, 1996), and the plant-like vacuole or vacuolar compartment (PLV or VAC) (Miranda *et al.*, 2010, Parussini *et al.*, 2010). Acidocalcisomes are electron-dense organelles with a high content of polyphosphate (polyP), calcium, magnesium, sodium, and zinc (Docampo & Moreno, 2011, Lander *et al.*, 2016). The PLV is similar to the lysosome of other cells, and to the vacuole of plants. Both acidocalcisomes and the PLV are acidified by two proton pumps, the vacuolar proton pyrophosphatase (TgVP1) and the vacuolar proton ATPase (V-ATPase) (Liu *et al.*, 2014, Stasic *et al.*, 2019). These acidic Ca^{2+} stores can take up Ca^{2+} driven by a proton gradient but the mechanism of Ca^{2+} release is unknown (Miranda *et al.*, 2010). The importance of acidocalcisomes and the PLV in Ca^{2+} signaling and homeostasis in *T. gondii* is still not completely clear.

PolyP consists of a linear arrangement of inorganic orthophosphates connected by high-energy phosphoanhydride bounds (Xie & Jakob, 2019). Despite its simplicity in structure, polyP has an outstanding number of important functions in all cells (Xie & Jakob, 2019). PolyP accumulates in acidocalcisomes, and their synthesis is accomplished through the activity of a vacuolar transporter chaperone (VTC) complex (Hothorn *et al.*, 2009) that hydrolyzes ATP to synthesize and translocate polyP inside the lumen of the organelle (Docampo & Moreno, 2011). Due to the inherently negative charge, polyP is often complexed with various cations including Ca^{2+} (Docampo *et al.*, 2005). Yeasts express 5 known proteins that form part of the VTC complex (VTC1-5) (Desfougeres *et al.*, 2016), but genetic evidence from *Toxoplasma* supports the presence of only two subunits, VTC2 (TgGT1_298630) and VTC4 (TGGT1_299080). VTC2 is an integral membrane protein that is part of the VTC complex but has also been postulated to play a role in vacuole fusion (Müller *et al.*, 2002). VTC4 is also believed to play a role in vacuole fusion and is the catalytic subunit of the VTC complex responsible for the polymerization of polyP (Müller *et al.*, 2002, Hothorn *et al.*, 2009). A previous study showed that TgVTC2 is important for *T. gondii* virulence and localizes to punctate spots within the cytosol of both intracellular and extracellular tachyzoites that did not colocalize with micronemes, rhoptries, dense granules or plant-like vacuole markers (Rooney *et al.*, 2011). TgVTC4 has not been characterized in *T. gondii*.

The V-ATPase is a multisubunit enzyme that couples the hydrolysis of ATP with the translocation of H^+ across membranes (Forgac, 2007). In previous work in *T. gondii,* we demonstrated that the V-ATPase localizes to the plasma membrane where it is involved in proton extrusion and maintenance of the membrane potential, and to endosome-like compartments, where it is involved in the maturation of rhoptry and microneme proteins (Stasic *et al.*, 2019). Disruption of the V-ATPase *a*1 subunit (Vha1), which is present in the membrane anchoring V_0 domain, led to a strong growth defect, affecting all the major steps of the lytic cycle (Stasic *et al.*, 2019).

Ca^{2+} transport by Ca^{2+} pumps is linked to proton transport (Schwiening *et al.*, 1993a, Bublitz *et al.*, 2013), and changes in membrane potential are linked to ion fluxes (Åkerman, 1978), hence in this work we studied the role of proton transport in Ca^{2+} entry and release from intracellular stores. We investigated how disruption of the *T. gondii* V-ATPase impacted Ca^{2+} homeostasis and signaling. We found that the integrity of the V-ATPase is necessary for the regulation of Ca^{2+} entry, maintenance of

a normal steady-state $[Ca^{2+}]_c$, Ca^{2+} storage in the ER, and acidic stores, as well as in Ca^{2+} signaling involved in parasite motility and egress from its host cell.

Results

Proton transport impacts Ca^{2+} entry at the plasma membrane

We first investigated if defective proton transport at the plasma membrane affected Ca^{2+} influx. We previously demonstrated that downregulating the expression of the *T. gondii* Vha1 subunit of the V-H^+-ATPase with anhydrotetracycline (ATc), disturbed the function of the whole complex resulting in defective proton extrusion, pH recovery and plasma membrane potential (Stasic *et al.*, 2019). All these defects were recovered by complementing the Vha1 subunit in the *iΔvha1-HA-CM* mutant. We used the *iΔvha1-HA* mutant, which was either grown in the absence of ATc (control) or with ATc for 0, 2, or 3 days. The *iΔvha1-HA-CM* mutant (complemented) was grown with ATc. All cell lines were loaded with Fura 2-AM to study cytosolic Ca^{2+} changes (Fig. 1). We first tested Ca^{2+} entry by adding 1.8 mM Ca^{2+} to suspensions of extracellular tachyzoites previously incubated in a buffer containing 100 μM EGTA (< 50 nM intracellular Ca^{2+}) (Pace *et al.*, 2014) (Fig. 1A, B). These concentrations simulate the changes in $[Ca^{2+}]$ to which tachyzoites are exposed when they are intracellular (cytosol of host cells is less than 100 nM) vs extracellular (physiological extracellular $[Ca^{2+}]$ is around 1.5-2 mM (Clapham, 2007). Under these conditions, control parasites expressing a fully functional V-ATPase (*iΔvha1-HA*-ATc, or complemented cells, *iΔvha1-HA-CM*, +ATc) showed cytosolic Ca^{2+} increase, which was rapidly returned to basal levels (Fig. 1A, *inset, blue* and *green* tracings, respectively). However, mutant parasites previously exposed to ATc were unable to return cytosolic Ca^{2+} to basal levels. This was especially remarkable in cells exposed to ATc for 3 days (Fig. 1A-B). We quantified the $[Ca^{2+}]_{cyt}$ at 400 and 600 sec after adding extracellular Ca^{2+} (Supplemental Table S1) and found a significant difference between the *Δvha1-HA+ATc* mutant compared to control and complemented parasites. At 600 sec all cell lines showed $[Ca^{2+}]_{cyt}$ below 1 μM but it was significantly elevated in the mutant (2 days and 3 days with ATc). Measurement of the $\Delta[Ca^{2+}]_c$ at 900 sec after the addition of extracellular Ca^{2+} showed that the mutant had an average $\Delta[Ca^{2+}]_c$ of 19.0 ± 4.0 nM Ca^{2+},

and the complemented parasites (*iΔvha1-HA-CM*) had an average $\Delta[Ca^{2+}]_c$ of 34.0 ± 10.2 nM Ca^{2+}. Parasites incubated with ATc for 2 or 3 days had average $\Delta[Ca^{2+}]_c$ of 189 ± 11.1 and 1,090.9 ± 80.0 nM Ca^{2+}, respectively, after addition of extracellular Ca^{2+} (Fig. 1A-B). These extended cytosolic Ca^{2+} measurements showed that while parasites cultured with ATc for 2 days are able to control cytosolic Ca^{2+}, it is evident that in both cases (2 and 3 days + ATc) Ca^{2+} influx is enhanced (Fig. 1B).

To investigate whether the defective Ca^{2+} influx resulted in changes in resting steady-state Ca^{2+} levels we measured the cytosolic Ca^{2+} concentration of the *iΔvha1-HA* mutant treated with ATc for 2 or 3 days, to compare with the control (-ATc) and complemented cells (Fig. 1C). Interestingly, when proton transport was disturbed by downregulating the V-ATPase (*iΔvha1-HA* (+ATc) cells), there was a significant decrease in the resting cytosolic Ca^{2+} concentration of *iΔvha1-HA* (+ATc) cells, which was recovered in the *iΔvha1-HA-CM* mutant. Note that the reduced cytosolic Ca^{2+} (Fig. 1C) was observed when the parasites were suspended in a buffer without extracellular Ca^{2+}. This phenotype is not evident when the extracellular Ca^{2+} is at mM levels.

These results indicate that proton transport at the plasma membrane regulates Ca^{2+} influx, possibly by controlling the parasite plasma membrane potential (Stasic *et al.*, 2019) or by coupling H^+ ejection with Ca^{2+} influx (Schwiening *et al.*, 1993b) by the plasma membrane Ca^{2+}/H^+ counter-transporting ATPase TgA1 (Luo *et al.*, 2001).

Proton transport is important for storing Ca^{2+} by acidic stores and the ER

We next investigated how disrupting proton transport affected Ca^{2+} uptake by intracellular Ca^{2+} stores. With this aim, we measured cytosolic Ca^{2+} fluctuations in Fura 2-AM-loaded cells in response to triggers known to affect acidic Ca^{2+} stores. Addition of 10 mM NH_4Cl, which was shown previously to cause an increase in cytosolic Ca^{2+} by its release from acidic stores (Moreno & Zhong, 1996) caused an increase in cytosolic Ca^{2+} in control cells (-ATc). This increase was almost completely abolished in the V-ATPase mutant (+ATc) (Fig. 2A, *red* line). Interestingly, the response to thapsigargin (TG, 1 μM) was also reduced. TG blocks the sarco/endoplasmic reticulum Ca^{2+}-ATPase (SERCA) resulting in uncompensated Ca^{2+} leakage into the cytosol by an unknown mechanism (Moreno & Zhong, 1996, Thastrup *et al.*, 1990). This effect was also evident when reverting the order of additions (Fig. 2B). In both cases, addition of TG resulted in a cytosolic Ca^{2+}

increase that was significantly lower for the *iΔvha1-HA* mutant (+ATc) (Figs. 2A, B, *red* traces and columns).

We next tested bafilomycin A_1 (1 μM), an inhibitor of the V-ATPase. The addition of bafilomycin A_1 to control cells (-ATc) resulted in a small cytosolic Ca^{2+} increase (Fig. 2C). However, adding bafilomycin A_1 after TG resulted in a significantly higher increase of cytosolic Ca^{2+} (Fig. 2D). These results suggested that Ca^{2+} released from the ER by the effect of TG was taken up by the bafilomycin A_1-sensitive Ca^{2+} stores and support the role of the ER as a highly efficient Ca^{2+} store that can also act in replenishing other Ca^{2+} stores. In contrast, bafilomycin A_1 did not release significant amounts of Ca^{2+} in the *iΔvha1-HA* mutant (+ATc), even after the addition of TG, in agreement with the absence of a functional V-ATPase (Fig. 2C, D).

We finally tested the lysosomotropic agent glycyl-L-phenylalanine-naphthylamide (GPN), which mobilizes Ca^{2+} from acidic organelles (Haller *et al.*, 1996, Lloyd-Evans *et al.*, 2008, Miranda *et al.*, 2010, Yuan *et al.*, 2021). Addition of GPN to *T. gondii* tachyzoites caused an increase in cytosolic Ca^{2+} which is significantly reduced in the *iΔvha1*(+ATc) mutant (Fig. 2E, F). The effect of TG following the addition of GPN shows that both stores are independent of each other but also that the store(s) where GPN acts on is actively recruiting Ca^{2+} from the ER. The reverse is also the case. This is seen in the increased response observed when either GPN or TG is added second. In both experimental conditions reduced proton transport of the mutant resulted in a reduced response.

In summary, these results demonstrate that the proton transport activity of the V-ATPase is important for the storage of Ca^{2+} by acidic compartment and most interesting the data indicate an interaction and exchange of Ca^{2+} between the ER and acidic organelles.

Proton transport is important for polyP content of acidocalcisomes

Acidocalcisomes are a major store of polyP and Ca^{2+} (Moreno & Zhong, 1996, Docampo & Moreno, 2011, Docampo *et al.*, 2005). We previously showed that inhibition of the V-ATPase by bafilomycin A_1 resulted in Ca^{2+} release from acidocalcisomes, which was associated with polyP hydrolysis (Rodrigues *et al.*, 2002). These observations suggested an association between the proton gradient generated by the V-ATPase, Ca^{2+} storage, and polyP content.

As synthesis of polyP occurs through the activity of the Vacuolar Transporter Chaperone complex (VTC), which uses ATP as energy source (Gerasimaitė *et al.*, 2014), we investigated whether the V-ATPase co-localizes with the VTC complex to acidocalcisomes. We C-terminally tagged the *T. gondii* VTC4 (TgVTC4, TgGT1_299080), which is the catalytic subunit of the VTC complex (Hothorn *et al.*, 2009), with a Ty1 epitope in the *iΔvha1-HA* strain. Immunofluorescence analysis (IFA) showed that VTC4 appears as small puncta (Fig. 3A), suggesting acidocalcisome localization, and VTC4-Ty1 co-localized with Vha1-HA (Fig. 3A *arrows*). We also observed co-localization and contact of acidocalcisomes with the plant-like vacuole (PLV) (Fig. 3B, and *inset*), confirming previous observations in which both organelles were shown to be in close contact (Miranda *et al.*, 2010). Acidocalcisomes are electron-dense organelles of approximately 200 nm in diameter and can be easily seen by direct transmission electron microscopy (EM) of whole tachyzoites (Luo *et al.*, 2001). We found that when the V-ATPase was disrupted, the acidocalcisomes became less electron-dense and/or reduced in numbers as compared to control parasites (Figs. 3C, D). We found a significant reduction in polyP levels after disrupting the V-ATPase (Fig. 3E). Short-chain polyp extracts from mutant and complemented lines were resolved in a 35% PAGE system to measure short chain polyP, which was significantly decreased in the *iΔvha1-HA*+ATc mutant. We had seen previously that KOs of the V-H^+-pyrophosphatase (*Δvp1*) impacted polyP levels (Miranda *et al.*, 2010). We extracted and quantified short chain polyP from *iΔvha1-HA* (+ and - ATc), *Δvp1*, *iΔvha1-HA-Δvp1*+ATc, and *iΔvha1-HA-CM*+ATc cells and observed that depletion of either the V-ATPase or VP1 resulted in significantly lower levels of endogenous polyPs (Fig. 3F). Interestingly, the *iΔvha1-HA-Δvp1* double mutant contained similar levels of polyP as the respective single mutants suggesting that disruption to either pump caused significant deficiencies in polyP synthesis and storage that were not additive (Fig. 3F). These data show that proton transport at the membrane of acidocalcisomes is important for polyP synthesis and storage which affects the capacity of the compartment to store Ca^{2+}.

Proton transport affects the Ca^{2+} signals that stimulate motility and egress

With the aim to study cytosolic Ca^{2+} in *T. gondii* intracellular stages we used genetically encoded Ca^{2+} indicators (GECIs) which are minimally invasive and therefore compatible with long term *in vivo* measurements. To investigate the connection between proton pumping by the V-ATPase and

Ca^{2+} signaling in *T. gondii* we engineered the *iΔvha1* mutant with a plasmid that expresses both GCaMP6f (Chen *et al.*, 2013) and mScarlet genes with a porcine teschovirus-1 (P2A) (Kim *et al.*, 2011) interspaced between both genes (Fig. S1A) (Vella *et al.*, 2020). Expression of both peptides permits ratiometric measurements of cytoplasmic Ca^{2+} in live cells. We isolated clones that we named *iΔvha1-HA-GmS*, and assayed them for growth and found that they did not show significant differences when compared with the parental cells with or without ATc (Fig. S1B). To ensure that the ratiometric system was being expressed during ATc addition and to confirm that it was not being degraded with the addition of ATc, immunoblots were done and shown in Fig. S1C. The GCaMP6f-3Ty1 and the mScarlet peptides were predicted to have molecular masses of 54 kDa, and 34 kDa, respectively, while the full-length molecular mass without ribosome skipping would be 88 kDa. We found minimal expression of the full-length peptide, suggesting that the P2A ribosome skipping system was working efficiently (Fig. S1C). Next, we observed live the *iΔvha1-HA-GmS* mutant incubated with or without ATc to confirm that the ratiometric system was working in live cells (Fig. S1D) and we used these cells to investigate two Ca^{2+} signaling-dependent processes, tachyzoite egress from host cells and gliding motility of extracellular parasites. Quantification of the green to red signals of the *iΔvha1-HA-GmS* clones resulted in lower green signal which indicates lower levels of free intracellular Ca^{2+}(Fig. S1E) and phenocopies the results with Fura-2-AM (Fig. 1C).

We had previously shown the presence of a cytosolic Ca^{2+} threshold that needed to be reached prior to the stimulation of motility and egress (Vella *et al.*, 2021). With the aim to investigate if the plasma membrane proton gradient was important for reaching the Ca^{2+} threshold for egress, we cultured the *iΔvha1-HA-GmS* clone in the presence or absence of ATc in confluent hTERT host cells on MatTek dishes and stimulated egress with Ca^{2+} agonists (Fig. 4A). Ca^{2+} agonists, such as ionomycin and Zaprinast, have been instrumental in understanding Ca^{2+} fluxes in *T. gondii* cytosol and their link to lytic cycle steps (Sidik *et al.*, 2016, Borges-Pereira *et al.*, 2015). After 30 sec of time-lapse, 100 nM of ionomycin or 25 μM Zaprinast were added to stimulate egress (Fig. 4A). Culturing the *iΔvha1-HA-GmS* clone with ATc resulted in a significant increase in the time to egress response to ionomycin (Figs. 4B, C) or to Zaprinast (Figs. 4D, E).

We next tested if the reason for the delayed egress was that intracellular parasites were not able to reach the cytosolic Ca^{2+} threshold. With the aim to determine the green-to-red ratio in each parasite

inside the parasitophorous vacuoles (PVs) (Fig. 5A), the *iΔvha1-HA-GmS* clone was exposed to 100 nM ionomycin, which resulted in an increase in Ca^{2+} (*green* signal), which was compared to the *red* signal (Fig. 5B). Control parasites (-ATc) showed an increase in the green fluorescence and eventually egressed (Fig. 5B). Parasites incubated with ATc also showed an increase in their ratio (Fig. 5B), but a large number of them failed to egress (Fig. 5B *no egress*). We quantified the individual tracings of all the parasites in the PV, and observed that the threshold of Ca^{2+} failed to be reached (Figs. 5C, D *dashed line*). Addition of 25 μM Zaprinast, resulted in similar results where the +ATc clones failed to egress and the ratio values were below the required Ca^{2+} threshold (Figs. 5E-G). Note that a few mutant parasites do egress and they reach the Ca^{2+} threshold although they take longer (Fig. 5F-G). This could be due to mechanical rupture of the PV and exposure of those parasites to high Ca^{2+} which will result in influx. These results support a role for the proton gradient generated by the V-ATPase in reaching the cytosolic Ca^{2+} threshold that precedes egress from the host. The delayed egress of the mutant could be explained by the lower cytosolic Ca^{2+} and/or the reduced Ca^{2+} content of the ER and acidic stores which we proposed to be responsible for the first peak of cytosolic Ca^{2+} that precedes egress (Vella *et al.*, 2021).

We transfected the *iΔvha1-HA* parasites with a plasmid that expresses tdTomato in the cytoplasm or used *iΔvha1-HA-GmS* and *iΔvha1-HA-GmS-CM* parasites (Fig. 6A). We stimulated motility adding 1.8 mM Ca^{2+} and tracked parasites by time-lapse (Fig. 6B). Using a new tracking algorithm developed to calculate parasite velocities (Fazli *et al.*, 2017), we found that disruption of the V-ATPase significantly reduced the average and maximum speed of parasites compared to controls or the complemented mutant (Figs. 6B, and C, and Supp. Video 1). We found that the average speed of *iΔvha1-HA* –ATc, *iΔvha1-HA* +ATc, and *iΔvha1-HA-CM* +ATc tachyzoites were 5.3, 1.28, and 3.8 μm/sec, respectively. Because Ca^{2+} induced motility was impacted in the VHa1 knockdowns, we assayed if a Ca^{2+} threshold would also play a role in the stimulation of motility. We stimulated *iΔvha1-HA-GmS* and *iΔvha1-HA-GmS-CM* parasites with 1.8 mM Ca^{2+} and measured the GCaMP6/msScarlet ratio at the start (before Ca^{2+} addition) and at the frame prior to movement, and determined that disruption of the proton pump reduced the amplitude change in the fluorescence ratio (Fig. 6D). The -ATc and CM parasites had an average change in fluorescence ratio of 0.57 and 0.55, respectively. The *iΔvha1-HA-GmS* parasites that did move more that 5 μm had an average change in

fluorescence ratio of 0.33 and those that failed to move or moved <5 μm had an average change in fluorescence ratio of -0.04. These data support an interaction between pthe roton gradient generated by the V-ATPase and the intensity of the Ca^{2+} signal that precedes stimulation of motility.

Discussion

In this study we report that proton efflux at the plasma membrane regulates Ca^{2+} entry, a phenomenon previously reported to occur through a plasma membrane Ca^{2+} channel (Pace *et al.*, 2014). Additionally, proton transport was important for cytosolic Ca^{2+} homeostasis by collaborating with the Ca^{2+} pumps in the efflux of Ca^{2+} from the cytosol. Deregulation of cytosolic Ca^{2+} impacted the generation of the Ca^{2+} signals needed for the stimulation of gliding motility and parasite egress from host cells. Defective proton transport also affected replenishing of acidic Ca^{2+} stores like the PLV and acidocalcisomes, which also affected their polyphosphate content. We used the V-ATPase conditional mutant generated in our previous work (Stasic *et al.*, 2019) for these studies. This mutant was previously shown to be defective in proton transport at the plasma membrane, as measured by proton extrusion, intracellular pH recovery, and membrane potential. In addition, previous work from our lab showed proton transport stimulated by ATP and inhibited by bafilomycin in both PLV enriched fractions (Miranda *et al.*, 2010) and purified acidocalcisomes (Rohloff *et al.*, 2011).

The alteration of the proton transport activity affected the ability of the plasma membrane to regulate cytosolic Ca^{2+}. This was seen not only because of the increased and unregulated entry from the extracellular environment but also because the cytosolic Ca^{2+} was lower in the absence of extracellular Ca^{2+}. This phenotype was different from the one observed with the sodium hydrogen exchanger (NHE) mutant which had their cytosolic Ca^{2+} elevated even in the presence of EGTA (Arrizabalaga *et al.*, 2004). The increased Ca^{2+} entry caused by the disruption of the V-ATPase when cells are exposed to high extracellular Ca^{2+} levels (normal conditions) could be explained by the requirement of proton extrusion to maintain the membrane potential. It is well established that Ca^{2+} enters the tachyzoite in a highly regulated manner through plasma membrane channels and this influx is partially sensitive to inhibitors of voltage-operated Ca^{2+} channels (Pace *et al.*, 2014). It is possible that one of these channels could be activated by changes in membrane potential, which is controlled by H^+ gradients in *T. gondii* (Moreno *et al.*, 1998). Changes in the membrane potential have been

linked to Ca^{2+} influx in mammalian cells (Behringer & Segal, 2015). Voltage-operated Ca^{2+} channels are activated by membrane depolarization due to an increase in the open probability of the Ca^{2+} channel (Dolphin, 2021). In addition, Ca^{2+} removal from the parasite is coupled to H^+ uptake by the Ca^{2+}/H^+ counter-transporting Ca^{2+}-ATPase TgA1 of the plasma membrane. A defective proton extrusion by disruption of the V-ATPase would result in an increase in the concentration of H^+ at the cytosolic side of the plasma membrane altering the Ca^{2+}/H^+ exchange activity of the Ca^{2+}-ATPase resulting in uncompensated Ca^{2+} influx.

The SERCA-type Ca^{2+}-ATPase, which pumps Ca^{2+} into the ER, and TgA1, which localizes to acidocalcisomes and the plasma membrane (Luo *et al.*, 2005), are Ca^{2+} pumps known to exchange Ca^{2+} with H^+ (Bublitz *et al.*, 2013). These enzymes would be less active if the concentration of H^+ at the membrane of those organelles is increased. We observed a reduced effect of thapsigargin on the cytosolic Ca^{2+} efflux caused by inhibition of the SERCA-type Ca^{2+}-ATPase. If the SERCA is less functional at the membrane of the ER this would result in a reduced ER Ca^{2+} level. Moreover, disruption of the V-ATPase from acidic stores would result in alkalization of the organelles making Ca^{2+} uptake by the Ca^{2+}-ATPases also difficult.

Ca^{2+} signaling depends on transient Ca^{2+} increases due to its release from intracellular stores or uptake through the plasma membrane and would be affected if the stores are depleted and Ca^{2+} entry is defective. For example, two peaks of Ca^{2+} increase have been detected in parasites egressing from host cells, the first attributed to Ca^{2+} release from intracellular stores, and the second due to Ca^{2+} entry from the extracellular medium (Vella *et al.*, 2021). A cytosolic Ca^{2+} threshold had to be reached for the stimulation of motility and egress (Vella *et al.*, 2021). The data presented in this work showed that proton gradients are directly linked to the *T. gondii* cytosolic Ca^{2+} increase required for egress and stimulation of motility. Both Ca^{2+} influx and release from stores are impacted by the activity of the V-H^+-ATPase justifying the delayed egress and decreased motility of the mutant. It is possible that the decrease in average speed is linked to the decrease in the number of motility boosts/calcium transients as previously proposed (Wetzel *et al.*, 2004).

The electron dense appearance of acidocalcisomes, which result from concentrated polyPs bound to cations, facilitates their observation and counting by transmission electron microscopy (Miranda *et al.*, 2008). Our results showed that both polyP content and number of acidocalcisomes were reduced

when proton transport was abolished. In this regard, polyP synthesis in isolated vacuoles of *Dictyostelium discoideum* (possibly acidocalcisomes (Marchesini *et al.*, 2002)) is inhibited by the proton motive force (PMF) inhibitor carbonylcyanide m-chlorophenylhydrazone (CCCP) (Gomez-Garcia *et al.*, 2004) and polyP synthesis and translocation to the acidocalcisome-like vacuole of *Saccharomyces cerevisiae* are driven by the V-ATPase-dependent electrochemical gradient across the vacuolar membrane (Gerasimaitė *et al.*, 2014). Recent reports have shown that polyP is involved in the cell cycle (Henry & Crosson, 2013, Boutte *et al.*, 2012). Although replication was impacted in V-ATPase disrupted parasites (Stasic *et al.*, 2019), deletion of VP1 in *T. gondii* resulted in lower levels of polyP but without a replication phenotype (Liu *et al.*, 2014).

Previous work localized the V-ATPase to the plasma membrane, PLV, and immature rhoptries of *T. gondii* (Stasic *et al.*, 2019). Additional vesicles were also observed that were not identified. We previously showed proton pumping activity in acidocalcisome fractions stimulated by ATP (Rohloff *et al.*, 2011) but labeling of acidocalcisomes with specific markers has been a challenge due to the lack of specific protein markers, as VP1 also localizes to the PLV. The best evidence for the presence of acidocalcisomes in *T. gondii* was transmission EM and polyP measurements (Luo *et al.*, 2001). We present in this work the first demonstration of the co-localization of the *T. gondii* V-ATPase with VTC4, a subunit of the polyP synthesis complex, present in acidocalcisomes of other parasites (Docampo & Moreno, 2011). We believe that VTC4 is the first specific marker for *T. gondii* acidocalcisomes.

In summary, our data demonstrate that the PLV and acidocalcisomes, in conjunction with the ER, play an active role in storing Ca^{2+} and that the proton gradient generated by the activity of the V-ATPase is critically important for this function. We also demonstrate that the proton gradient generated at the plasma membrane by the V-ATPase plays a role in Ca^{2+} influx, likely through maintaining the membrane potential or by coupling with the Ca^{2+}-ATPase. Finally, we demonstrate a link between Ca^{2+}, pH, and polyP that is important for the lytic cycle of *T. gondii*.

Materials and methods

Chemicals, reagents, and cell cultures.

Fura 2-AM was obtained from Invitrogen (Life Technologies, Inc.). Anhydrotetracycline (ATc), thapsigargin (TG), bafilomycin A_1, calcium chloride, ammonium chloride, and ionomycin (iono) were purchased from Sigma Aldrich. Glycyl-L-phenylalanine-naphthylamide (GPN) was from Santa Cruz biotech. HFF or hTERT (human telomerase reverse transcriptase) cells were maintained in Dulbecco's modified Eagle medium (DMEM) with 10% cosmic calf serum at 37°C with 5% CO_2. *Toxoplasma gondii* strains *iΔvha1-HA, iΔvha1-HA-CM,* and *TATiΔku80* parasites were used in this study and were cultured as described (Stasic *et al.*, 2019, Fox *et al.*, 2009, Sheiner *et al.*, 2011).

Genetic manipulations.

iΔvha1-HA parasites were transfected with a plasmid that contained GCaMP6-Ty1-P2A-mScarlet-3xHA and FACS sorted by both green and red fluorescence. Stable clones (termed *iΔvha1-HA-GmS)* were selected with a good dynamic range of green fluorescence upon addition of extracellular Ca^{2+}. Plaque assays and western blot controls were performed to ensure that the genetically encoded Ca^{2+} indicator did not impact parasite growth. To create the complemented cell line, Vha1 cDNA was introduced into the *uprt* gene locus as previously described (Stasic *et al.*, 2019). Verification of insertion was confirmed via immunoblot and PCR (data not shown). Stable clones of *iΔvha1-HA-GmS-vha1* (termed *GmS-CM*) were selected and were found to be able to grow in the presence of ATc. Vacuolar transporter chaperone 4 (VTC4; TGGT1_299080) was C-terminally tagged with a Ty1 epitope in the *iΔvha1-HA* strain using the CRISPR protospacer GCCAACGTTTCGGCAGCCGA. Primers 5' ctgcaaattgacgcgggagttaaaaaactgaagtcggtaatgcgtgaattggatgcattg 3' and 5' aaggaagcaagtcacggcaccatcgagcagggagaggaaccatcctgcaagtgcatagaa 3' were used to amplify 40 base pairs of homology upstream and downstream of the translational stop codon and 3Ty1-DHFR from a template tagging plasmid. This strain was termed *iΔvha1-HA-VTC4-Ty1*.

Measuring intracellular Ca^{2+} with Fura 2-AM.

Intracellular Ca^{2+} was determined fluorometrically by loading parasites with Fura 2-AM as described previously (Moreno & Zhong, 1996, Vella *et al.*, 2020). Briefly, parasites were harvested, washed with buffer A with glucose (BAG; 116 mM NaCl, 5.4 mM KCl, 0.8 mM $MgSO_4$, 50 mM

Hepes, pH 7.3, and 5.5 mM glucose), and filtered through a 5 μm filter. Parasites were resuspended to 1 x 10^9 parasites/ml in BAG + 1.5% sucrose with 5 μM Fura 2-AM. Parasite suspensions were incubated for 26 min in a 26°C water bath with mild agitation. Cells were washed twice with BAG to remove the extracellular dye and were resuspended at a final density of 1 x 10^9 cells/ml. A 50 μL aliquot of this suspension was added to 2.45 mL of Ringer buffer (155 mM NaCl, 3 mM KCl, 1 mM $MgCl_2$, 3 mM NaH_2PO_4, and 10 mM Hepes, and 10 mM dextrose) in a cuvette that is placed in a thermostatically controlled Hitachi F-7100 fluorescence spectrophotometer. The excitation wavelength was set at 340 and 380 nm, and emission at 510 nm. The Fura2 fluorescence was calibrated from the ratio of 340/380 nm fluorescence values after subtraction of the background fluorescence of the cells at 340 and 380 nm as described by Grynkiewicz et al. (Grynkiewicz *et al.*, 1985). Concentration of $[Ca^{2+}]$i was calculated by employing an iterative computer program that is part of the Hitachi 7000 software (Grynkiewicz *et al.*, 1985). The maximum and minimun $[Ca^{2+}]$ are measured prior to each experiment and for each cell line and the values entered in the equation described by Grynkiewicz et al. to establish the linear range of the concentration vs fluorescence relationship. *i*Δ*vha1-HA* and *i*Δ*vha1-HA-CM* parasites were incubated with ATc for 0, 2, or 3 days and loaded with Fura 2-AM. Quantification of changes in $[Ca^{2+}]_c$ was performed by measuring the change between the initial and final Ca^{2+} concentration. Thapsigargin (TG), bafilomycin A_1 and other agonists were added at the indicated times and concentrations indicated in the figure legends. Quantifications of the slopes were determined by the increase in fluorescence during the first 10-20 sec after addition of Ca^{2+} ionophores or Ca^{2+} agonists. 3-6 independent trials were performed for quantifications. To determine the initial Ca^{2+} levels in Fura 2-AM loaded parasites, the initial Ca^{2+} readings from suspensions were determined from 4-6 independent trials averaging the first 50 sec of each tracing.

Measuring intracellular Ca^{2+} with GCaMP6f.

The *i*Δ*vha1-HA-GmS* strain was used for these measurements (Kim *et al.*, 2011). *i*Δ*vha1-HA-GmS* parasites were incubated with ATc for 0, 2, or 3 days and viewed under an Olympus IX-71 inverted fluorescence microscope with a Photometrix CoolSnapHQ CCD camera driven by DeltaVision software. The exposure duration, gain, laser intensity, and filter settings were identical for all images taken for quantification. DeltaVision Softworx software was used to measure pixel intensity of red and green signals of individual parasites (averaged per PV) in 4-6 independent

experiments. The ratio of green-to-red fluorescence in parasites was used to quantify relative intracellular calcium levels.

Chemical induced parasite egress.

Twenty-four hours prior to egress experiments, parasites were inoculated onto confluent hTERT host cells 30 mm MatTek dishes. Egress was triggered with 100 nM ionomycin or 25 μM Zaprinast, which were added at 30 sec of the time -lapse and videos were allowed to record for up to 15 min. Images were acquired by time-lapse microscopy with identical settings for each of the 6 independent trials. In each field of view, the time post addition of the stimulant until the first evidence of parasite egress from a PV was enumerated. The first 5 quickest egressing PVs were averaged for each independent trial. If $\leq$ 5 PVs showed no parasite egress, each PV (up to 5 total) was assigned the maximum time of the time-lapse (15 min). For each independent trial, the individual fluorescence values of red and green signal of all the members of the PV was recorded. The ratio of green-to-red signal was determined for the individual parasites that either egressed or did not egress. To quantify the relative level of Ca^{2+} required for egress, the ratios from all members of the same PV were averaged and the averaged values of 4-6 independent trials (per PV) are reported.

PolyP and acidocalcisome analysis.

Short-chain polyP from 1 x 10^9 parasites were extracted as previously described (Ruiz *et al.*, 2001) with some modifications. First, *iΔvha1-HA*, *Δvp1*, *iΔvha1-HAΔvp1,* and *iΔvha1-HA-CM* were incubated with or without ATc for 3 days and were washed with BAG. Extraction of short-chain polyP was done with ice-cold $HClO_4$ (0.5 M) according to the published protocol (Ruiz *et al.*, 2001) for resolution in a 35 % polyacrylamide gel (Cordeiro *et al.*, 2019). For polyP quantification, we used 10^8 parasites and quantification of polyP levels was determined using the malachite green assay to measure phosphate release by yeast exopolyphosphatase, as described previously (Lanzetta *et al.*, 1979). For electron microscopy, parasites were washed and placed on copper grids, which were allowed to air dry (Luo *et al.*, 2001). Once dried, parasites were imaged on a transmission electron microscope JEOL JEM1011. Images were randomized and assayed double-blinded. Quantification of acidocalcisomes were from 2 independent trials where a total of 67 -ATc and 57 +ATc cells were

enumerated. Immunofluorescence microscopy was performed as previously described (Stasic *et al.*, 2019) on *iΔvha1-HA-VTC4-Ty1*. Rat-anti-HA (1:25) and mouse-anti-Ty1 (1:1,000) were used to probe the localization of acidocalcisomes.

Motility analysis.

Changes in motility of the parasites were determined as previously described (Borges-Pereira *et al.*, 2015) with some modifications. tdTomato-expressing or GCaMP6f-2PA-mScarlet parasites grown with or without ATc were used to visualize motility or quantify Ca^{2+} levels. Twenty four hours prior to microscopy, 35 mm MatTek dishes were incubated with 10% FBS to provide sufficient protein to form a surface conducive to motility. MatTek dishes were washed once with PBS and loaded with 2 ml of Ringer buffer without Ca^{2+}. MatTek dishes were chilled on ice, parasites were added to the dish and allowed to equilibrate for 15 min. Dishes were then placed in the Zeiss LSM 710 Confocal Microscope environmental chamber set at 37°C. 1.8 mM Ca^{2+} was added and motility was imaged and quantified as previously described (Fazli *et al.*, 2017). Briefly, for each independent trial, the average and maximum observed speed were determined, each individual parasite speed was sorted from highest to lowest, and the top 20 highest speeds per independent trial were used to determine quantification. There were 3 or 4 independent trials of *i*Δ*vha1-HA*–ATc, *i*Δ*vha1-HA* +ATc, and *i*Δ*vha1-HA-CM* +ATc assayed in this fashion. For measuring relative Ca^{2+} levels, *i*Δ*vha1-HA* or *i*Δ*vha1-HA-CM* GCaMP6f-2PA-mScarlet expressing parasites were used. The ratio of green-to-red fluorescence before the addition of 1.8 mM $CaCl_2$ and the frame before the parasite movement (where movement is defined as a distance traveled greater than 5 μm) was determined and the change in the ratio reported. Data from 3 independent trials and the change in fluorescence ratio of 10 parasites per trial are reported.

Computational motility tracking.

We developed a novel computational tracking program to locate, follow, and quantify *T. gondii* in videos without any manual intervention. We based our tracking model based on the Kanade Lucas Tomasi (KLT) approach (Rehg, 1995), which operates by detecting "salient" features, or features relevant to the unique object identification, using the Tomasi algorithm. KLT uses the "optical flow"

(Shin, 2005) method for extracting the most important features of the cells, generating a bounding box to enclose the features of interest, and finally tracking the center of mass of the bounding boxes across the video. KLT makes use of pixel intensity information to search for fluorescence patterns that yield the best match in terms of corresponding objects. To mitigate occlusions (objects passing in front of or behind each other), we designed a post-processing module and used Kalman filters (Kalman, 1960). Kalman filters predict future events based on past events, building an historical "momentum" to maintain object correspondence, even when that object is occluded by another. Kalman filters work well for single cell tracking, but in the case of tracking multiple cells, we needed an additional algorithm for linking detected cells in the current frame to their corresponding cells in the previous frame. We used the Hungarian Algorithm (Frank, 2005), which combined with our tracking module, was able to detect all the cells' trajectories across time.

We implemented our pipeline using Python 3.5 and associated scientific computing libraries (NumPy, SciPy, scikit-learn, scikit-image, and Matplotlib). The core of our tracking algorithm used a combination of tools available in the OpenCV 3.1 computer vision library. The full code for our pipeline will be soon available under the MIT open-source license. We have deployed variants of this tracking method in 2D and 3D fluorescence videos of *T. gondii* (Fazli *et al.*, 2017, Fazli, 2018a, Fazli, 2018b, Fazli, 2019).

Statistical analysis.

All statistical analyses were performed using GraphPad Prism. Unless otherwise noted, all error bars are presented as the standard error of the mean (SEM) and from a minimum of three independent trials. Differences were considered significant if P values were < 0.05.

Acknowledgment

The authors thank the Georgia Electron microscopy core facilities for the EM images taken during this study and Dr. Muthugapatti Kandasamy and the Biomedical Microscopy Core of the University of Georgia for the use of the microscopes. This work was supported by the U.S. National Institutes of Health grants AI096836 and AI128356 to SNJM. The computer work was partially supported by a Google research grant to use on their Computer Platform. We acknowledge partial support from the

NSF Advances in Biological Informatics (ABI) CAREER ABI-Innovation under award number 1845915 to SQ. AJS, SAV and MSF were partially supported through fellowships directly funded by a T32 training grant, 5T32AI060546 or through fellowships awarded by the Office of Research to support the T32 training goals.

Conflict of interest

The authors declare that they have no conflicts of interest with the contents of this article.

Data availability statement

All data generated or analyzed in this study are included in this published article (and its supplementary information files).

References

Åkerman, K.E.O. (1978) Changes in membrane potential during calcium ion influx and efflux across the mitochondrial membrane. *Biochimica et Biophysica Acta (BBA) - Bioenergetics* **502**: 359-366.

Ambroise-Thomas, P., and Pelloux, H. (1993) Toxoplasmosis — congenital and in immunocompromised patients: A parallel. *Parasitology Today* **9**: 61-63.

Arrizabalaga, G., Ruiz, F., Moreno, S., and Boothroyd, J.C. (2004) Ionophore-resistant mutant of *Toxoplasma gondii* reveals involvement of a sodium/hydrogen exchanger in calcium regulation. *The Journal of Cell Biology* **165**: 653.

Behringer, E.J., and Segal, S.S. (2015) Membrane potential governs calcium influx into microvascular endothelium: integral role for muscarinic receptor activation. *The Journal of physiology* **593**: 4531-4548.

Black, M.W., and Boothroyd, J.C. (2000) Lytic Cycle of *Toxoplasma gondii*. *Microbiology and Molecular Biology Reviews* **64**: 607.

Blader, I.J., Coleman, B.I., Chen, C.T., and Gubbels, M.J. (2015) Lytic Cycle of Toxoplasma gondii: 15 Years Later. *Annu Rev Microbiol* **69**: 463-485.

Borges-Pereira, L., Budu, A., McKnight, C.A., Moore, C.A., Vella, S.A., Triana, M.A.H., Liu, J., Garcia, C.R., Pace, D.A., and Moreno, S.N. (2015) Calcium Signaling throughout the *Toxoplasma gondii* Lytic Cycle a study using genetically encoded calcium indicators. *Journal of Biological Chemistry* **290**: 26914-26926.

Boutte, C.C., Henry, J.T., and Crosson, S. (2012) ppGpp and Polyphosphate Modulate Cell Cycle Progression in *Caulobacter crescentus*. *Journal of Bacteriology* **194**: 28.

Bublitz, M., Musgaard, M., Poulsen, H., Thogersen, L., Olesen, C., Schiott, B., Morth, J.P., Moller, J.V., and Nissen, P. (2013) Ion pathways in the sarcoplasmic reticulum Ca2+-ATPase. *J Biol Chem* **288**: 10759-10765.

Chen, T.-W., Wardill, T.J., Sun, Y., Pulver, S.R., Renninger, S.L., Baohan, A., Schreiter, E.R., Kerr, R.A., Orger, M.B., Jayaraman, V., Looger, L.L., Svoboda, K., and Kim, D.S. (2013) Ultrasensitive fluorescent proteins for imaging neuronal activity. *Nature* **499**: 295-300.

Clapham, D.E. (2007) Calcium signaling. *Cell* **131**: 1047-1058.

Cordeiro, C.D., Ahmed, M.A., Windle, B., and Docampo, R. (2019) NUDIX hydrolases with inorganic polyphosphate exo- and endopolyphosphatase activities in the glycosome, cytosol and nucleus of Trypanosoma brucei. *Biosci Rep* **39**.

Desfougeres, Y., Gerasimaite, R.U., Jessen, H.J., and Mayer, A. (2016) Vtc5, a Novel Subunit of the Vacuolar Transporter Chaperone Complex, Regulates Polyphosphate Synthesis and Phosphate Homeostasis in Yeast. *J Biol Chem* **291**: 22262-22275.

Docampo, R., de Souza, W., Miranda, K., Rohloff, P., and Moreno, S.N.J. (2005) Acidocalcisomes - conserved from bacteria to man. *Nature Reviews Microbiology* **3**: 251.

Docampo, R., and Moreno, S.N.J. (2011) Acidocalcisomes. *Cell Calcium* **50**: 113-119.

Dolphin, A.C. (2021) Functions of Presynaptic Voltage-gated Calcium Channels. *Function (Oxf)* **2**: zqaa027.

Fazli, M.S., Vella, S.A., Moreno, S.N., and Quinn, S. (2017) Computational motility tracking of calcium dynamics in *Toxoplasma gondii*. *arXiv preprint arXiv:1708.01871*.

Fazli, M.S.S., R.V.; Alaila, B.; Vella, S.A.; MorenoS.N.J.; Ward, G.E.; QUinn, S. (2019) Lightweight and Scalable Particle Tracking and Motion Clustering of 3D Cell Trajectories. *2019 IEEE International Conference on Data Science and Advanced Analytics (DSAA)*: 412-421.

Fazli, M.S.V., Stephen A.; Moreno, S.N.J.; Quinn, Shannon (2018a) Unsupervised discovery of toxoplasma gondii motility phenotypes. *2018 IEEE 15th International Symposium on Biomedical Imaging* **ISBI 2018**.

Fazli, M.S.V., Stephen A.; Moreno, S.N.J.; Ward, Gary E.; Quinn, Shannon (2018b) Toward Simple & Scalable 3D Cell Tracking. *2018 IEEE International Conference on Big Data (Big Data)* 3217-3225.

Forgac, M. (2007) Vacuolar ATPases: rotary proton pumps in physiology and pathophysiology. *Nat Rev Mol Cell Biol* **8**: 917-929.

Fox, B.A., Ristuccia, J.G., Gigley, J.P., and Bzik, D.J. (2009) Efficient gene replacements in *Toxoplasma gondii* strains deficient for nonhomologous end joining. *Eukaryot Cell* **8**: 520-529.

Frank, A. (2005) On Kuhn's Hungarian method a tribute from Hungary. *Naval Research Logistics (NRL)* **52.1**: 2-5.

Gerasimaitė, R., Sharma, S., Desfougères, Y., Schmidt, A., and Mayer, A. (2014) Coupled synthesis and translocation restrains polyphosphate to acidocalcisome-like vacuoles and prevents its toxicity. *Journal of Cell Science* **127**: 5093.

Gomez-Garcia, M.R., Ruiz-Perez, L.M., Gonzalez-Pacanowska, D., and Serrano, A. (2004) A novel calcium-dependent soluble inorganic pyrophosphatase from the trypanosomatid Leishmania major. *FEBS Lett* **560**: 158-166.

Grynkiewicz, G., Poenie, M., and Tsien, R.Y. (1985) A new generation of Ca2+ indicators with greatly improved fluorescence properties. *J Biol Chem* **260**: 3440-3450.

Haller, T., Dietl, P., Deetjen, P., and Völkl, H. (1996) The lysosomal compartment as intracellular calcium store in MDCK cells: a possible involvement in InsP3-mediated Ca^{2+} release. *Cell Calcium* **19**: 157-165.

Henry, J.T., and Crosson, S. (2013) Chromosome replication and segregation govern the biogenesis and inheritance of inorganic polyphosphate granules. *Molecular Biology of the Cell* **24**: 3177-3186.

Holland, G.N. (1989) Ocular toxoplasmosis in the immunocompromised host. *International Ophthalmology* **13**: 399-402.

Hortua Triana, M.A., Márquez-Nogueras, K.M., Vella, S.A., and Moreno, S.N.J. (2018) Calcium signaling and the lytic cycle of the Apicomplexan parasite *Toxoplasma gondii*. *Biochimica et Biophysica Acta (BBA) - Molecular Cell Research* **1865**: 1846-1856.

Hothorn, M., Neumann, H., Lenherr, E.D., Wehner, M., Rybin, V., Hassa, P.O., Uttenweiler, A., Reinhardt, M., Schmidt, A., Seiler, J., Ladurner, A.G., Herrmann, C., Scheffzek, K., and Mayer, A. (2009) Catalytic core of a membrane-associated eukaryotic polyphosphate polymerase. *Science* **324**: 513-516.

Kalman, R.E. (1960) A New Approach to Linear Filtering and Prediction Problems. *Journal of Basic Engineering* **82**: 35-45.

Kim, J.H., Lee, S.-R., Li, L.-H., Park, H.-J., Park, J.-H., Lee, K.Y., Kim, M.-K., Shin, B.A., and Choi, S.-Y. (2011) High Cleavage Efficiency of a 2A Peptide Derived from Porcine Teschovirus-1 in Human Cell Lines, Zebrafish and Mice. *PLOS ONE* **6**: e18556.

Lander, N., Cordeiro, C., Huang, G., and Docampo, R. (2016) Polyphosphate and acidocalcisomes. *Biochem Soc Trans* **44**: 1-6.

Lanzetta, P.A., Alvarez, L.J., Reinach, P.S., and Candia, O.A. (1979) An improved assay for nanomole amounts of inorganic phosphate. *Analytical Biochemistry* **100**: 95-97.

Liu, J., Pace, D., Dou, Z., King, T.P., Guidot, D., Li, Z.-H., Carruthers, V.B., and Moreno, S.N.J. (2014) A vacuolar-H^+-pyrophosphatase (TgVP1) is required for microneme secretion, host cell invasion, and extracellular survival of *Toxoplasma gondii*. *Molecular Microbiology* **93**: 698-712.

Lloyd-Evans, E., Morgan, A.J., He, X., Smith, D.A., Elliot-Smith, E., Sillence, D.J., Churchill, G.C., Schuchman, E.H., Galione, A., and Platt, F.M. (2008) Niemann-Pick disease type C1 is a sphingosine storage disease that causes deregulation of lysosomal calcium. *Nat Med* **14**: 1247-1255.

Lourido, S., and Moreno, S.N.J. (2015) The calcium signaling toolkit of the Apicomplexan parasites *Toxoplasma gondii* and *Plasmodium* spp. *Cell Calcium* **57**: 186-193.

Luo, S., Ruiz, F.A., and Moreno, S.N.J. (2005) The acidocalcisome Ca^{2+}-ATPase (TgA1) of *Toxoplasma gondii* is required for polyphosphate storage, intracellular calcium homeostasis and virulence. *Molecular Microbiology* **55**: 1034-1045.

Luo, S., Vieira, M., Graves, J., Zhong, L., and Moreno, S.N.J. (2001) A plasma membrane-type Ca^{2+}-ATPase co-localizes with a vacuolar H^+-pyrophosphatase to acidocalcisomes of *Toxoplasma gondii*. *The EMBO Journal* **20**: 55.

Machala, L., Kodym, P., Malý, M., Geleneky, M., Beran, O., and Jilich, D. (2015) Toxoplasmosis in immunocompromised patients. *Epidemiol Mikrobiol Imunol* **64**: 59-65.

Marchesini, N., Ruiz, F.A., Vieira, M., and Docampo, R. (2002) Acidocalcisomes are functionally linked to the contractile vacuole of Dictyostelium discoideum. *J Biol Chem* **277**: 8146-8153.

Miranda, K., Pace, D.A., Cintron, R., Rodrigues, J.C.F., Fang, J., Smith, A., Rohloff, P., Coelho, E., De Haas, F., De Souza, W., Coppens, I., Sibley, L.D., and Moreno, S.N.J. (2010)

Characterization of a novel organelle in *Toxoplasma gondii* with similar composition and function to the plant vacuole. *Molecular Microbiology* **76**: 1358-1375.

Miranda, K., Souza, W.d., Plattner, H., Hentschel, J., Kawazoe, U., Fang, J., and Moreno, S.N.J. (2008) Acidocalcisomes in Apicomplexan parasites. *Experimental Parasitology* **118**: 2-9.

Moreno, N.J.S., Zhong, L., Lu, H.-G., Souza, W.D.E., and Benchimol, M. (1998) Vacuolar-type H^+-ATPase regulates cytoplasmic pH in *Toxoplasma gondii* tachyzoites. *Biochemical Journal* **330**: 853.

Moreno, S.N.J., and Zhong, L. (1996) Acidocalcisomes in *Toxoplasma gondii* tachyzoites. *Biochemical Journal* **313**: 655.

Müller, O., Bayer, M.J., Peters, C., Andersen, J.S., Mann, M., and Mayer, A. (2002) The Vtc proteins in vacuole fusion: coupling NSF activity to V_0 *trans*-complex formation. *The EMBO Journal* **21**: 259.

Pace, D.A., McKnight, C.A., Liu, J., Jimenez, V., and Moreno, S.N.J. (2014) Calcium Entry in *Toxoplasma gondii* and Its Enhancing Effect of Invasion-linked Traits. *Journal of Biological Chemistry* **289**: 19637-19647.

Parussini, F., Coppens, I., Shah, P.P., Diamond, S.L., and Carruthers, V.B. (2010) Cathepsin L occupies a vacuolar compartment and is a protein maturase within the endo/exocytic system of *Toxoplasma gondii*. *Molecular Microbiology* **76**: 1340-1357.

Patel, S., and Docampo, R. (2010) Acidic calcium stores open for business: expanding the potential for intracellular Ca2+ signaling. *Trends Cell Biol* **20**: 277-286.

Rehg, J.M., Kanade, Takeo (1995) Model-based tracking of self-occluding articulated objects. *Computer Vision*.

Rodrigues, C.O., Ruiz, F.A., Rohloff, P., Scott, D.A., and Moreno, S.N.J. (2002) Characterization of Isolated Acidocalcisomes from *Toxoplasma gondii* Tachyzoites Reveals a Novel Pool of Hydrolyzable Polyphosphate. *Journal of Biological Chemistry* **277**: 48650-48656.

Rohloff, P., Miranda, K., Rodrigues, J.C.F., Fang, J., Galizzi, M., Plattner, H., Hentschel, J., and Moreno, S.N.J. (2011) Calcium Uptake and Proton Transport by Acidocalcisomes of *Toxoplasma gondii*. *PLOS ONE* **6**: e18390.

Rooney, P.J., Ayong, L., Tobin, C.M., Moreno, S.N.J., and Knoll, L.J. (2011) TgVTC2 is involved in polyphosphate accumulation in *Toxoplasma gondii*. *Molecular and Biochemical Parasitology* **176**: 121-126.

Ruiz, F.A., Rodrigues, C.O., and Docampo, R. (2001) Rapid changes in polyphosphate content within acidocalcisomes in response to cell growth, differentiation, and environmental stress in Trypanosoma cruzi. *J Biol Chem* **276**: 26114-26121.

Schwiening, C.J., Kennedy, H.J., and Thomas, R.C. (1993a) Calcium-hydrogen exchange by the plasma membrane Ca-ATPase of voltage-clamped snail neurons. *Proc Biol Sci* **253**: 285-289.

Schwiening, C.J., Kennedy, H.J., and Thomas, R.C. (1993b) Calcium-hydrogen exchange by the plasma membrane Ca-ATPase of voltage-clamped snail neurons. *Proceedings of the Royal Society B* **253**: 285-289.

Sheiner, L., Demerly, J.L., Poulsen, N., Beatty, W.L., Lucas, O., Behnke, M.S., White, M.W., and Striepen, B. (2011) A systematic screen to discover and analyze apicoplast proteins identifies a conserved and essential protein import factor. *PLoS Pathog* **7**: e1002392.

Shin, J.K., Sangjin; Kang, Sangkyo; Lee Seaon-Won; Paik, Joonki; Abidi, Besma, Abidi, Mongi. (2005) Optical flow-based real-time object tracking using non-prior training active feature model. *Real-Time Imaging* **11**.

Sidik, S.M., Hortua Triana, M.A., Paul, A.S., El Bakkouri, M., Hackett, C.G., Tran, F., Westwood, N.J., Hui, R., Zuercher, W.J., Duraisingh, M.T., Moreno, S.N.J., and Lourido, S. (2016) Using a Genetically Encoded Sensor to Identify Inhibitors of *Toxoplasma gondii* Ca^{2+} Signaling. *Journal of Biological Chemistry* **291**: 9566-9580.

Stasic, A.J., Chasen, N.M., Dykes, E.J., Asady, B., Vella, S.A., Starai, V.J., and Moreno, S.N.J. (2019) The *Toxoplasma* Vacuolar H^+-ATPase regulates intracellular pH and impacts the maturation of essential secretory proteins. *Cell Reports* **27**: 2132-2146.e2137.

Thastrup, O., Cullen, P.J., Drøbak, B.K., Hanley, M.R., and Dawson, A.P. (1990) Thapsigargin, a tumor promoter, discharges intracellular Ca^{2+} stores by specific inhibition of the endoplasmic reticulum Ca^{2+}-ATPase. *Proceedings of the National Academy of Sciences* **87**: 2466.

Vella, S.A., Calixto, A., Asady, B., Li, Z.H., and Moreno, S.N.J. (2020) Genetic Indicators for Calcium Signaling Studies in Toxoplasma gondii. *Methods Mol Biol* **2071**: 187-207.

Vella, S.A., Moore, C.A., Li, Z.H., Hortua Triana, M.A., Potapenko, E., and Moreno, S.N.J. (2021) The role of potassium and host calcium signaling in Toxoplasma gondii egress. *Cell Calcium* **94**: 102337.

Wetzel, D.M., Chen, L.A., Ruiz, F.A., Moreno, S.N., and Sibley, L.D. (2004) Calcium-mediated protein secretion potentiates motility in Toxoplasma gondii. *J Cell Sci* **117**: 5739-5748.

Xie, L., and Jakob, U. (2019) Inorganic polyphosphate, a multifunctional polyanionic protein scaffold. *J Biol Chem* **294**: 2180-2190.

Yuan, Y., Kilpatrick, B.S., Gerndt, S., Bracher, F., Grimm, C., Schapira, A.H., and Patel, S. (2021) The lysosomotrope, GPN, mobilises Ca(2+) from acidic organelles. *J Cell Sci*.

FIGURE LEGENDS

FIGURE 1: Ca^{2+} entry is affected by the activity of the V-ATPase. A) Representative tracings of Fura 2-AM loaded *iΔvha1-HA* and *iΔvha1-HA-CM* extracellular tachyzoites previously grown with ATc for the indicated days. Tachyzoites were suspended in Ringer buffer with 100 μM EGTA and 1.8 mM $CaCl_2$ was added at 150 s (arrow). Inset shows an expanded Y scale of the first 500 sec. B) Quantification of the change in intracellular Ca^{2+} levels observed from 200-900s. Note that parasites cultured with ATc for 2 days show enhanced Ca^{2+} influx but they are still able to control cytosolic levels even at 900 sec. Parasites cultured for 3 d +ATc maintained cytosolic Ca^{2+} levels below 1 μM up to ~800sec. A-B Data are from 3-5 independent trials. B data were compared with one-way ANOVA test from 3 independent trials where $*P < 0.05$; $**P < 0.01$; $****P < 0.0001$. C)) Fura 2-AM loaded *iΔvha1-HA* and *iΔvha1-HA-CM* clones incubated with ATc for the indicated days. Data are reported as the average of the first 60 sec of basal Ca^{2+} levels from 6 independent trials. Panel C was compared with one-way ANOVA test, where $**P < 0.01$ and $****P < 0.0001$.

FIGURE 2: Ca^{2+} uptake by acidic stores is affected by the activity of the V-ATPase. Representative tracings of Fura 2-AM loaded extracellular tachyzoites. A) NH_4Cl (20 mM) and TG (1 μM) were added at 100 and 400 sec, respectively. B) Similar to A with the addition of reagents reversed. C) Bafilomycin A_1 (Baf, 1 μM) and TG (1 μM) were added at 100 and 400 seconds, respectively. D) Similar to C with the addition of reagents reversed. E) GPN (30 μM) and TG (1 μM) were added at 100 and 400 seconds, respectively. F) Similar to E with the addition of reagents reversed. Panels A-F used *iΔvha1-HA* and clones incubated with ATc for 0 or 3 days. A-G inset graphs show the quantification of the change in $[Ca^{2+}]_{cyt}$ levels between the level 10 seconds prior to the addition of the indicated compound and the maximum peak after addition. All measurements were done in Ringer buffer containing 100 μM EGTA. Panels A-F are from 3-4 independent trials using a student's T-test where $*P < 0.05$; $**P < 0.01$; n. s., not significant.

FIGURE 3: PolyP storage by acidocalcisomes and the activity of the V-ATPase. A) Super-resolution images of *iΔvha1-HA-VTC4-Ty1* extracellular tachyzoites showing Vha1 colocalization

with VTC4 (arrows in inset). B) Super-resolution images of *iΔvha1-HA-VTC4-Ty1* parasites showing Vha1 colocalization with VTC4, highlighting the association with the PLV (inset). Scale bars are 2 μm. Dashed lines are the outline of the parasite. C) Electron microscopy of whole cell *iΔvha1-HA* parasites. D) quantification of acidocalcisome number per parasite. Data are from 2 independent trials where a total of 67 -ATc and 57 +ATc were enumerated. E) Short chain polyP gel from *iΔvha1-HA* and *iΔvha1-HA-CM* parasites incubated with or without ATc on a 30% polyacrylamide gel. F) Quantification of short chain polyphosphate of *iΔvha1-HA*, *Δvp1*, *iΔvha1-HAΔvp1,* and *iΔvha1-HA-CM*. Panel F was compared with one-way ANOVA test, where ***$P < 0.001$, ****$P < 0.0001$.

FIGURE 4: Ca^{2+}-stimulated egress and the activity of the V-ATPase. A) Cartoon depicting the measurement of parasite egress. B) *iΔvha1-HA-GmS* clones were incubated with ATc for 0, 2 or 3 days (day 3 video not shown). After 30 sec of the time-lapse, 100 nM ionomycin was added. C) Quantification of the time to egress. Data are reported as the average time of the first parasite to egress from the first 5 parasitophorous vacuoles. D) *iΔvha1-HA-GC6-mS* clones were incubated with ATc for 0, 2, or 3 days (day 3 video not shown). After 30 sec of the time-lapse, 25 μM Zaprinast were added. E) Quantification of egress time. Data are reported as the average time of the parasite to egress from the first 5 parasitophorous vacuoles. For the purpose of clarity only the red channel is shown in panels B and D. Panels C and D were compared with one-way ANOVA test, *$P < 0.05$; **$P < 0.01$; ***$P < 0.001$, ****$P < 0.0001$.

FIGURE 5: A threshold for Ca^{2+} is required for egress. A) Cartoon showing the protocol for measurements of egress of individual parasites from a single parasitophorous vacuole in response to calcium agonists. B) *iΔvha1-HA-GmS* clones were incubated with ATc for 0, 2 or 3 days (day 3 video not shown). After 30 sec of the time-lapse, 100 nM ionomycin were added. Arrows indicated the addition of 100 nM ionomycin and the time of the egress of the first parasite. C) Representative tracings of the ratio of red to green fluorescence of all the parasites in a single parasitophorous vacuole. For clones incubated with ATc, some parasites failed to egress from the parasitophorous vacuole and a representative tracing is overlaid. Each frame represents 3 seconds. D) The peak ratio

observed before egress of all members of the parasitophorous vacuole were averaged into a single value of 6 independent trials. E) *iΔvha1-HA-GmS* clones were incubated with ATc for 0, 2, or 3 days (day 3 video not shown). F) After 30 sec of time-lapse, 25 μM Zaprinast were added. Arrows indicated the addition of 25 μM Zaprinast and the time of egress of the first parasite. Each frame represents 3 seconds. G) The peak ratio, prior to egress, of all members in the parasitophorous vacuole were averaged into a single value of 6 independent trials. One-way ANOVA was performed where $*P < 0.05$; $**P < 0.01$; $***P < 0.001$; $****P < 0.0001$.

FIGURE 6: Ca^{2+}-stimulated motility and the activity of the V-ATPase. A) Cartoon showing the protocol to measure Ca^{2+}-stimulated motility. B) Time-lapse microscopy where tdTomato expressing *iΔvha1-HA* and *iΔvha1-HA-CM* were incubated with or without ATc for 0 or 2 days. At the indicated time, 1.8 mM calcium was added. C) Motility assaying average speed or maximum (top speed) speed of tdTomato expressing *iΔvha1-HA* and *iΔvha1-HA-CM* with or without ATc. The motility of 40-80 individual parasites from 3 independent trials per clone were tracked and then sorted as fastest to slowest where the top 20 per independent trial were used for quantification. Displayed are the top 20 velocities (60 data points in total from 3 independent trials) per trial and clone. Error bars are SEM and data were analyzed by GraphPad Prism. D) Quantification of the change in ratio at the start of the time-lapse to one frame before movement of *iΔvha1-HA-GmS* and *iΔvha1-HA-GmS-CM* clones incubated with ATc for 0 or 2 days. One-way ANOVA was performed where $****P < 0.0001$.

FIGURE S1: Expressing a Genetic Calcium indicator in the V-ATPase mutant. A) Cartoon depicting the ratiometric GCaMP6-mScarlet construct. P, tubulin promoter; GCaMP6f, genetically encoded calcium indicator version 6-fast; Ty1, epitope tag; P2A, porcine teschovirus-1; HA, hemagglutinin. B) Plaque assay comparing the parental strain (*iΔvha1-HA*) and the *iΔvha1-HA-GmS* clone with or without ATc for 8 days. C) Western blots comparing parental strain (*iΔvha1-HA*) with the *iΔvha1-HA-GmS* clone with the addition of ATc for the indicated time. Note that we cropped the western blot so the signal for vha1 is not seen. The western shows that both GCaMP6 (Ty-tagged) and mScarlet (HA-tagged) are expressed as separate peptides instead of a single peptide and the ribosome skipping strategy is functional. Anti Ty1 1:1,000; Anti-HA 1:200; Anti-Tubulin 1:30,000. D) Live cell microscopy of *iΔvha1-HA-GmS* incubated with or without ATc for 2 days. Scale bars are 2 μm. E) Quantification of the ratio of red to green signal in cell in *iΔvha1-HA-GmS* clones incubated with ATc for the indicated times. One-way ANOVA was performed where ****$P < 0.0001$.

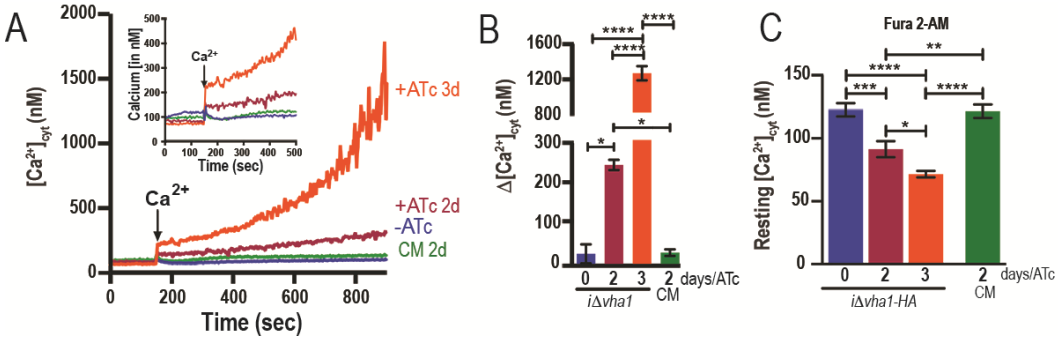

mmi_14722_f1.tif

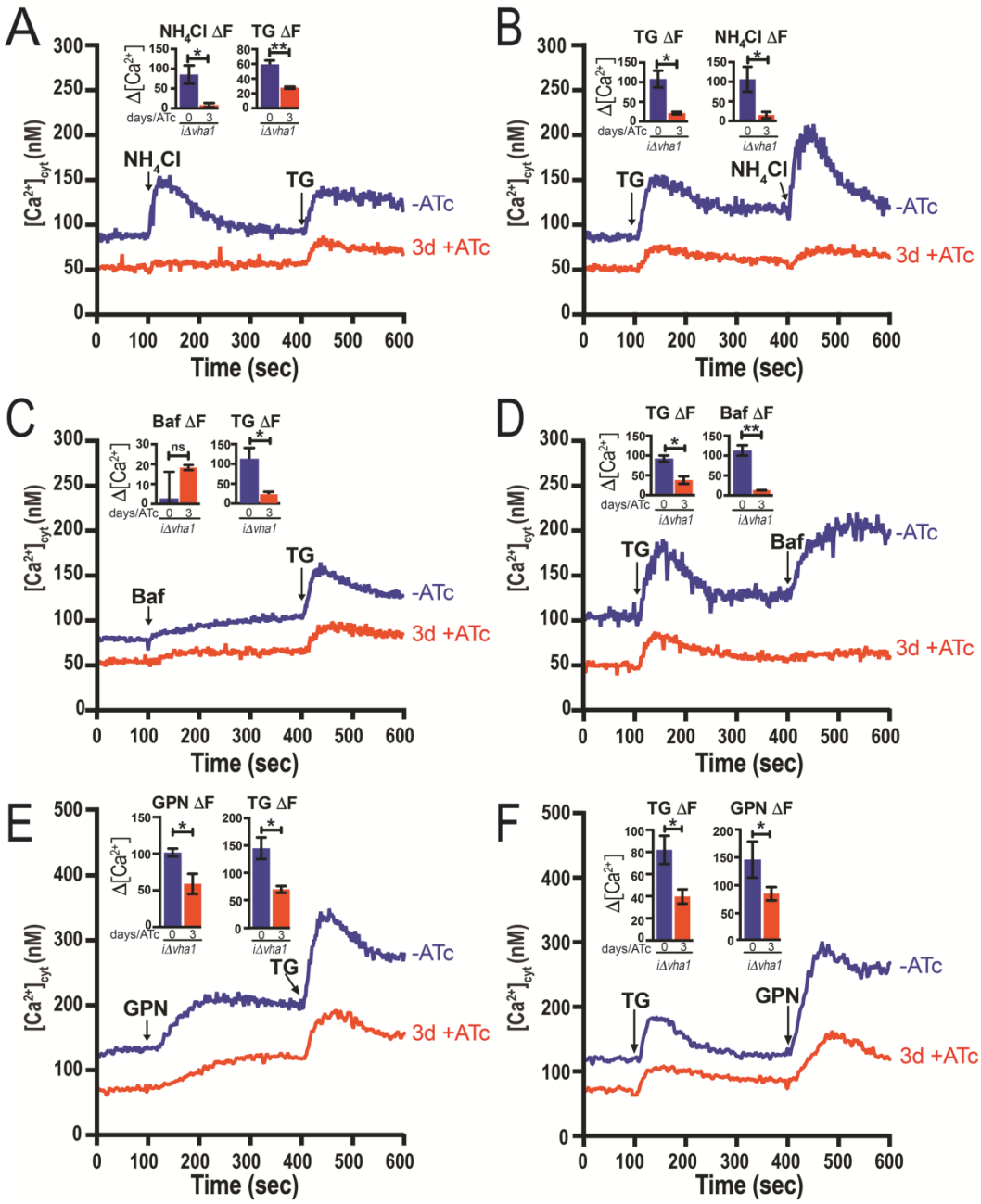

mmi_14722_f2.tif

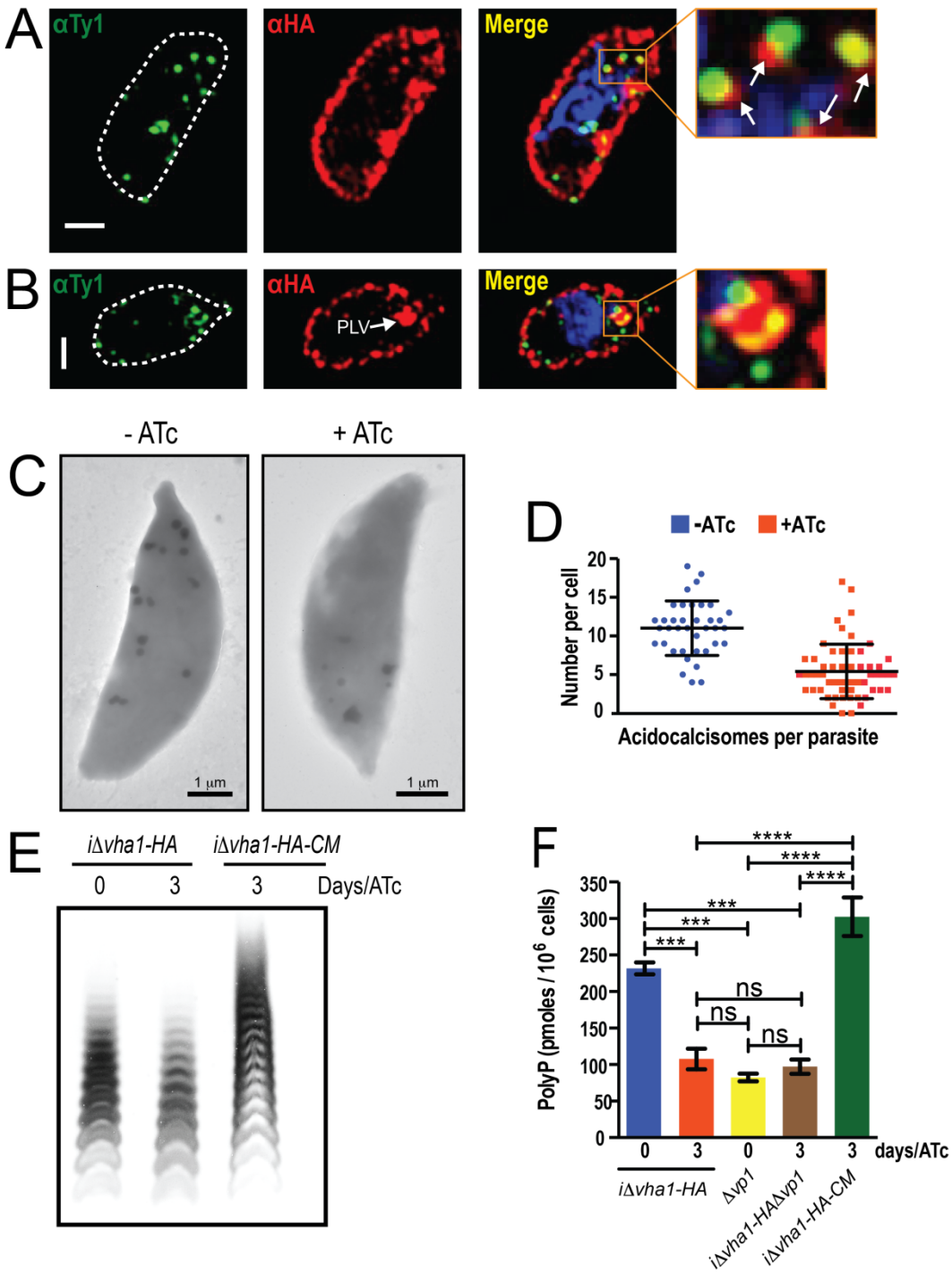

mmi_14722_f3.tif

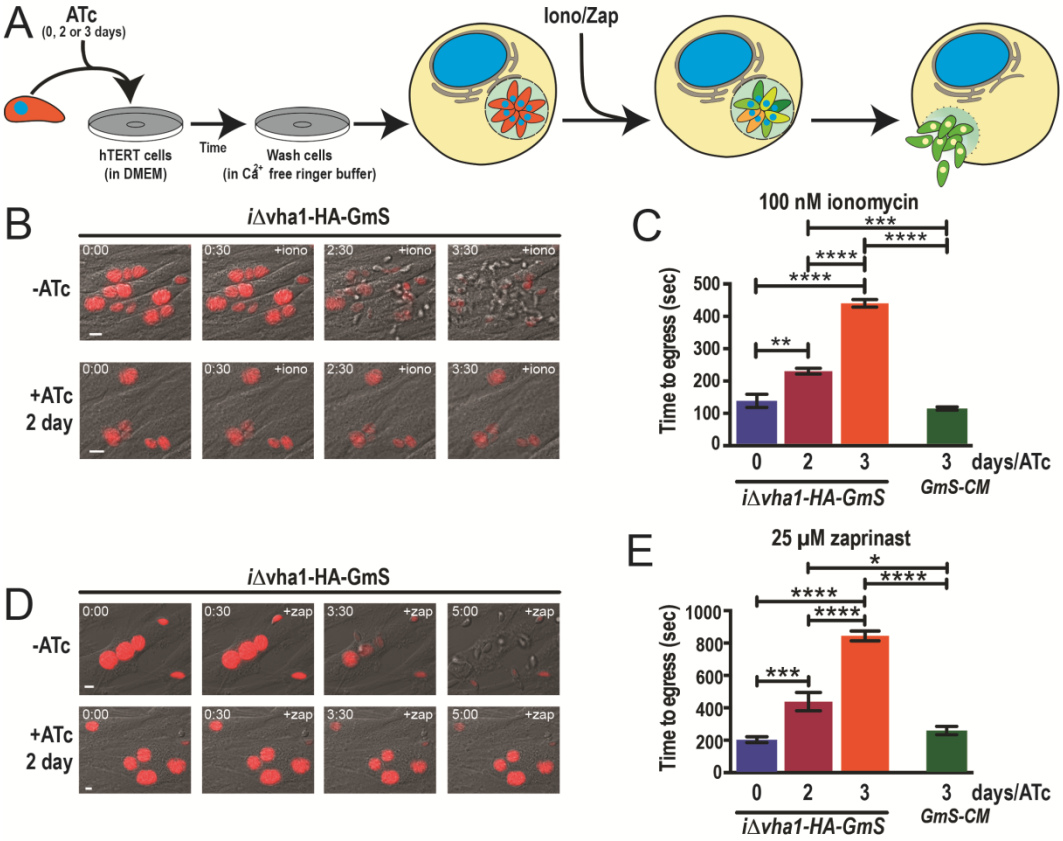

mmi_14722_f4.tif

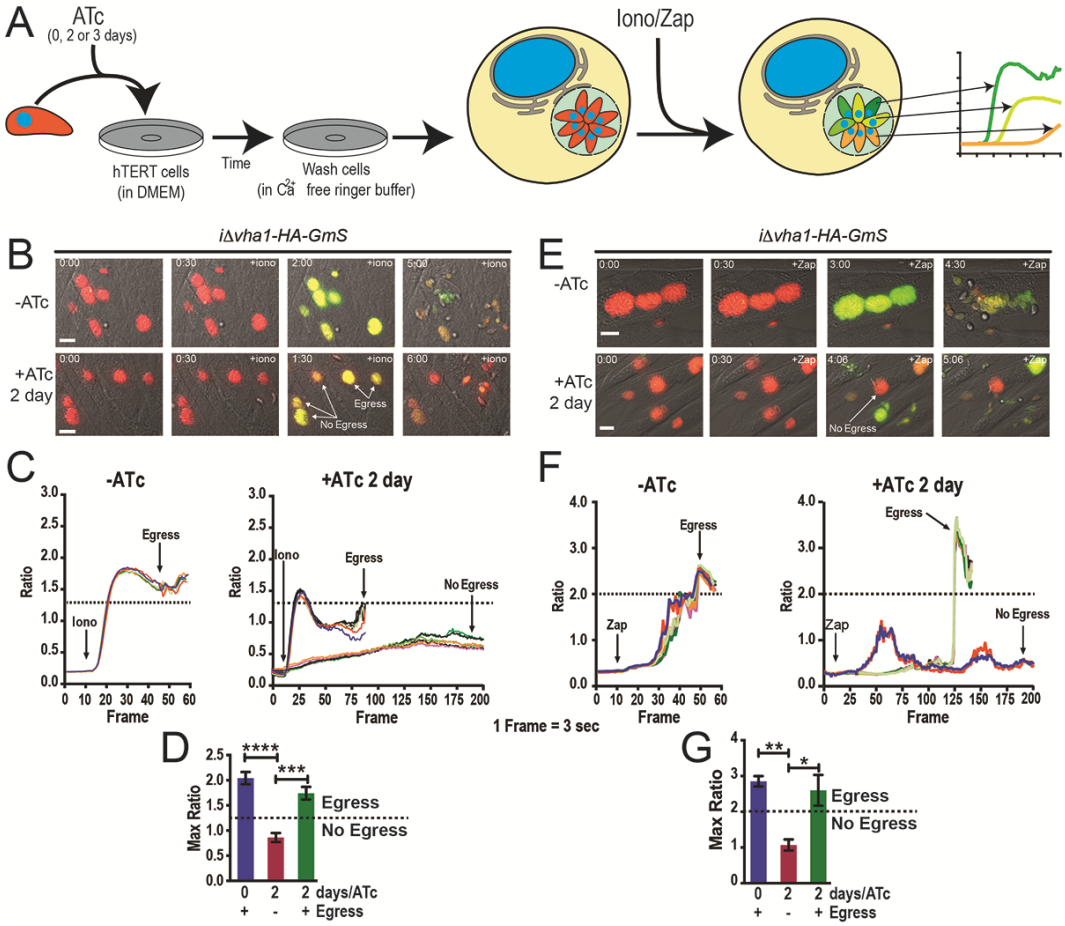

mmi_14722_f5.tif

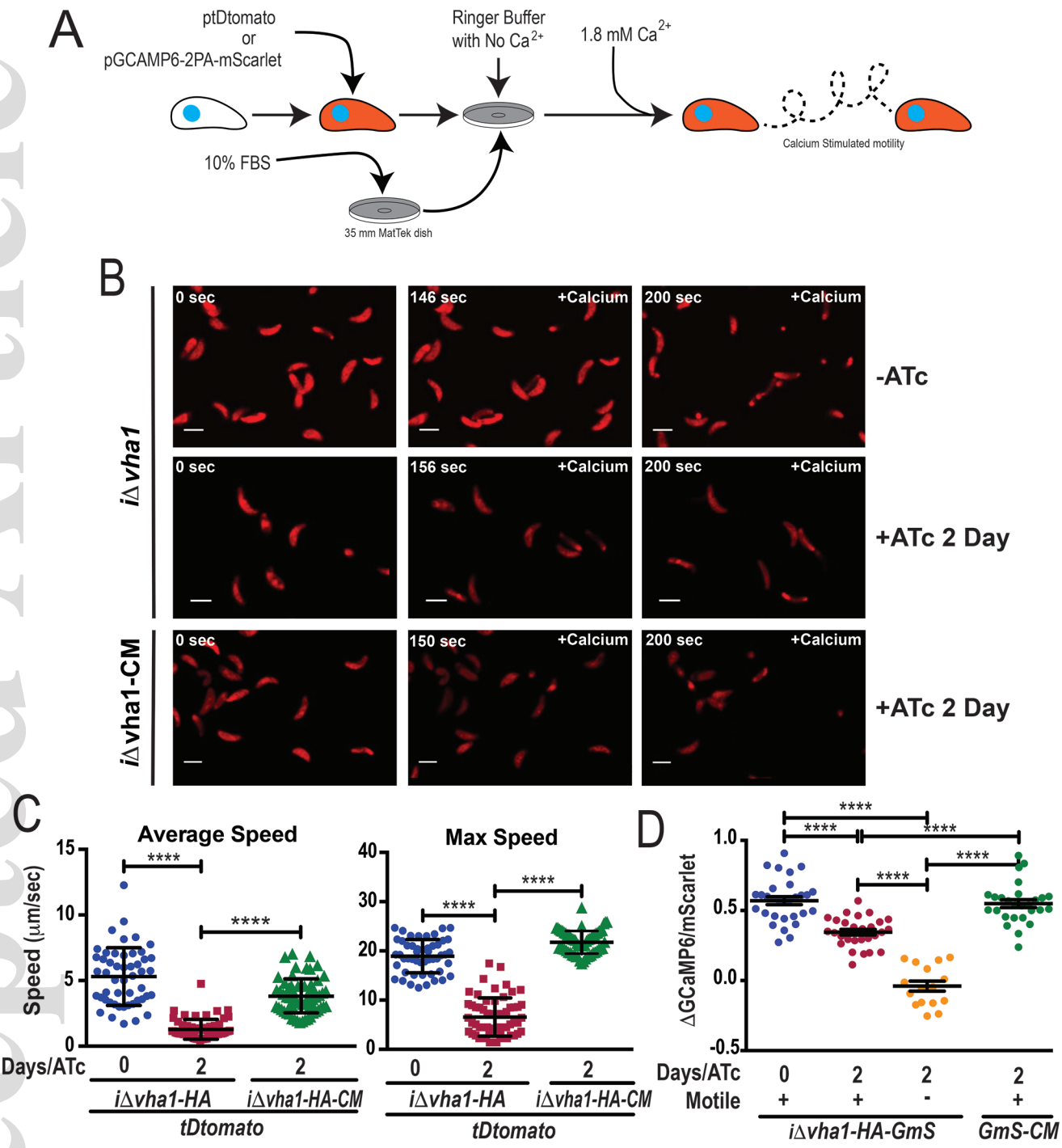

mmi_14722_f6.tif